Spring 2016

Solar Thermal Decoupled Electrolysis: Reaction Mechanism of Electrochemical Oxidation of CoO/Co(OH)2

William Prusinski
Valparaiso University

William Prusinski

Honors Candidacy in Chemistry: Final Report

CHEM 498

Advised by Dr. Jonathan Schoer

Solar Thermal Decoupled Electrolysis: Reaction Mechanism of Electrochemical Oxidation of $CoO/Co(OH)_2$

College of Arts and Sciences

Valparaiso University

Spring 2016

Abstract

A modified water electrolysis process has been developed to produce H_2. The electrolysis cell oxidizes CoO to CoOOH and Co_3O_4 at the anode to decrease the amount of electric work needed to reduce water to H_2. The reaction mechanism through which CoO becomes oxidized was investigated, and it was observed that the electron transfer occurred through both a species present in solution and a species adsorbed to the electrode surface. A preliminary mathematical model was established based only on the electron transfer to species in solution, and several kinetic parameters of the reaction were calculated. The average value of each parameter over six data points was as follows: the diffusion coefficient of the reduced species (D_R) was 1.03×10^{-3} cm^2/s, the electron transfer coefficient (α) was 0.49, the standard rate constant (k^o) was 6.87×10^{-6} cm/s, and reaction formal potential(E^o_f) was -0.284 V vs. Ag/AgCl. Based on poor results from curve fitting of experimental data obtained from chronoamperometry and cyclic voltammetry, it can be concluded that this model does not comprise the electrochemical system completely. Thus, the model should be updated to include the adsorbed species in the electron transfer step.

Introduction

Hydrogen has enormous potential as an alternative fuel for automobiles since it does not produce carbon dioxide, CO_2, when combusted. However, the primary commercial process for producing hydrogen generates CO_2 as a byproduct.[1] Furthermore the production of H_2 via water electrolysis processes requires more electrical energy input than the energy obtained from the combustion of the produced hydrogen.[2]

We have developed a two-step cycle that resolves both of these problems. The process for the emission free production of hydrogen with net energy available to consider the gas as a fuel is diagramed in Fig. 1. The electrolysis differentiates itself from commercial processes by introducing a metal oxide into the electrolytic cell.[3] During electrolysis, the metal oxide becomes oxidized, decreasing the required theoretical electrical potential to produce the gas below 1.2 V. Thus it becomes possible to produce H_2 with less electric energy input than is available from H_2 used in a fuel cell or combusted in order to put electric power on the grid. The oxidized material can be reduced back to its original state by exposure to high temperature. This thermal step can be performed with solar energy, ensuring the entire reaction cycle is free of carbon emissions.

There is necessarily some carbon production associated with the electric power used in the electrolysis, but as the electrical grid shifts towards ever greater renewable energy sources over time, the carbon footprint of our process will decrease accordingly.

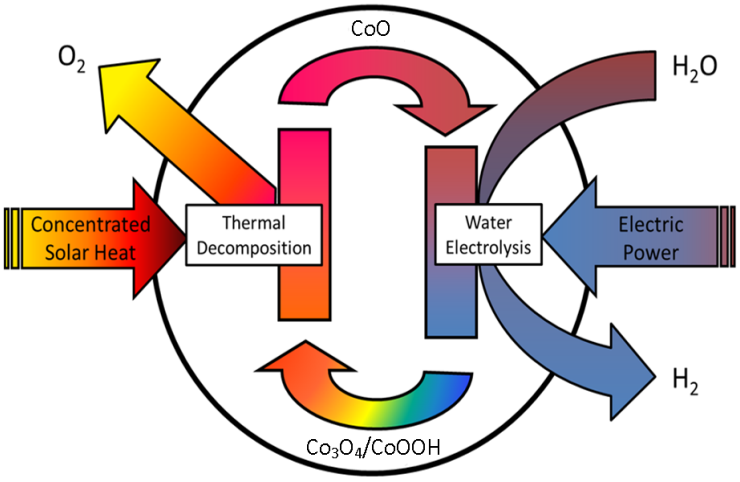

Figure 1. The two-step solar thermal electrolysis process for producing hydrogen.

This process must produce hydrogen at high current densities in order to be cost-effective and industrially competitive. Understanding the chemical mechanism is crucial for determining the reaction rates for the electrolysis so that the maximum current density can be achieved.

I will show that we have determined critical steps in the mechanism. Specifically, I show that the electroactive species being oxidized at the anode is $Co(OH)_2$ and the products are CoOOH and Co_3O_4. Furthermore I show that the electron transfer step likely occurs through an adsorption process for both the reduced and the oxidized species. I will also argue from exploratory experimental results that $Co(OH)_2$ in solution also undergoes the electron transfer step in parallel with the adsorption oxidation.

A major goal of the electrochemistry research is to obtain a quantitative understanding of the reaction steps so that a finite element model of the cell can be built, enabling us to glimpse into the industrial potential of the process. Such a model requires that we know fundamental

transport parameters like the diffusion coefficients of the electroactive species, the transfer coefficients at the anode as well as the specific rate constant or exchange current density for the anode reaction. The mathematical description of the adsorption process is quite complex, and even more so when coupled with an electron transfer to species in solution. Construction of a complete model requires more time and effort than could be allocated in this thesis, so I will outline different reaction mechanisms, some that account for this behavior, and some approximations that may serve as first time engineering estimates of potential cell performance. I thus describe mathematical models that enable quantitative interpretation of experimental results for the case where electron transfer occurs only from an electrode to an electroactive species in solution. The models enable us to connect experimental data to the transport parameters described above.

I understand that it is not likely that these models are adequate for our system, but two important results will emerge: (1) We will confirm or not confirm mathematically the importance of adsorption; (2) assuming the model is not adequate for ~~a~~accurate interpretation, it none-the-less becomes a starting point for building more complex models. The work presented is a necessary part of model building, therefore we make an important step towards uncovering the industrial potential of the process. I will also include some discussion of experimental techniques that we use in concert with our data-interpretation models, and I report some of the quantitative results obtained from our experimental work.

Furthermore, we recognize that a solid product forms on our anode and thus a complete mechanism at a very fundamental level needs to account for the formation of a solid phase and the influence this phase has on passivating the electrode. We do not expect to soon account for this phase growth and passivation effect. From an engineering point of view it may not be

necessary because it is clear that a real industrial process would need a means of cleaning the electrodes *in situ* to maintain an adequate current density.

In this thesis, I begin with a brief relevant history that shows the motivation for the research, develop a brief theoretical basis for interpreting experimental data, describe the models we have created for interpreting experimental results, discuss results both qualitative and quantitative, and end with a statement of future work.

Historical background

A proposed mechanism for the oxidation of cobalt oxide described by Elumalai et al is shown in Eq. 1.1-1.3.[4]

$$Co(OH)_2\ (solution) \rightarrow Co(OH)_2\ (surface) \quad 1.1$$
$$Co(OH)_2\ (surface) \rightarrow Co(OH)_2^+ + e^- \quad 1.2$$
$$Co(OH)_2^+ \rightarrow CoOOH + H^+ \quad 1.3$$

This mechanism was used during our preliminary work. However, the applicability of this mechanism was questioned for our system. We experienced a wide variability in the data between experimental campaigns as well as during a given experiment. We thus questioned our assumption that the reaction mechanism consisted of mass transfer of $Co(OH)_2$ to the anode followed by a one electron transfer step. To explain the variability in the data between and during experiments, we needed a more complex electrochemical mechanism.

In this paper, I argue that some of the added complexity is associated with the electroactive species, $Co(OH)_2$, being adsorbed on the electrode before it is oxidized, as well as the adsorption of the product, CoOOH. But there is a nuance: I will show that under some experimental conditions we see current vs changing potential data indicative of a diffusion step followed by the electron transfer step. Thus we are considering that parallel paths exist for the electrochemical oxidation of $Co(OH)_2$. We have supporting evidence for this hypothesis in the

form of cyclic voltammograms (CVs) and chronocoulometry responses, as well as support from the literature, which will be described in the next section.

We are in the process of using this information to update our mathematical models. I will describe the models in their current form in the theoretical background section, and show how we apply them to our experimental data in the results section.

Theoretical background

Fundamental principles of voltammetry

A distinctive feature of an adsorption reaction is a symmetrical peak in a CV as shown in Fig. 2.[5] The current starts low and rapidly rises as the potential increases. Because there is a limited amount of electroactive species adsorbed on the electrode, the current must reach a maximum. The current then drops to zero because all of the electroactive species are exhausted.

The amount of charge under the current vs. time curve is a fixed value dependent on the number of adsorption sites available on the electrode. Thus the scan rate of the CV will not impact the total charge. As the scan rate increases, however, the peak height increases linearly.[5]

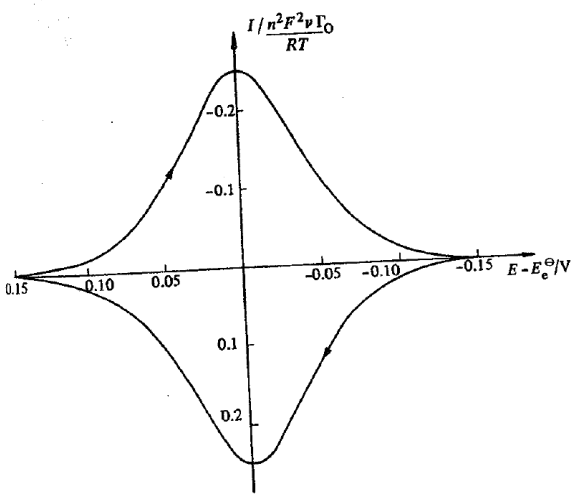

Figure 2. A typical CV peak for an adsorption reaction.

This behavior contrasts with a CV peak in a diffusion-controlled electrochemical process, in which the decreasing current decays in a non-symmetric manner, eventually leveling off to a non-zero value, seen in the CV shown in Fig. 3.[6]

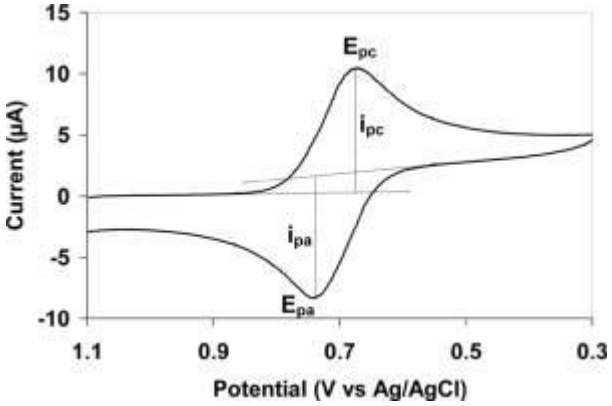

Figure 3. A typical CV peak for a diffusion-controlled reaction.

Like with the adsorption CV, the anodic current increases rapidly with increasing potential. But as that is occurring the concentration of the electroactive species at the electrode approaches zero. Once the concentration is zero, the current is completely dependent on the mass transfer condition within the cell. Specifically the current is dictated by the boundary layer thickness, which grows during the electrolysis until it reaches a steady state value. Fig. 4 shows how the boundary layer changes over time.[5] Once the boundary layer reaches a steady state, the current is completely dependent on the diffusion coefficient of the electroactive species, and thus remains constant. This condition is seen in Fig. 3 near 0.3 V.

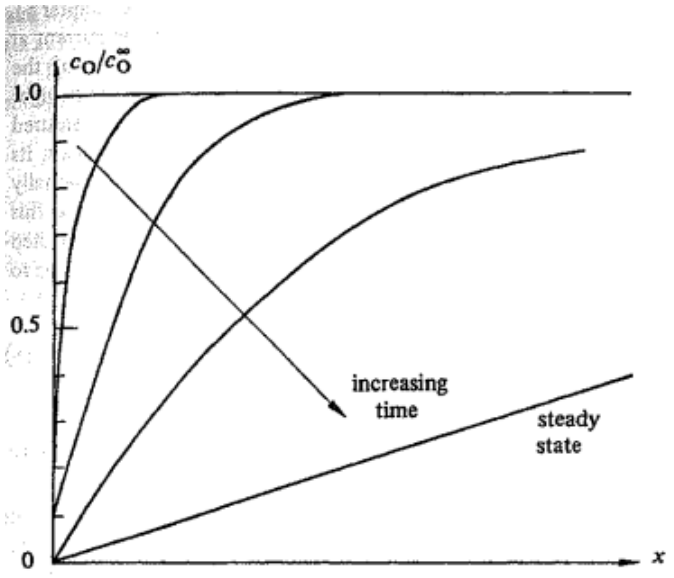

Figure 4. Ratio of the concentration of the electroactive species (C_O) over the concentration in the bulk solution (C_O^∞) as a function of distance from the electrode (x).

Thus the CV peak for diffusion has a different shape than that for adsorption. Furthermore, it can be shown mathematically that the peak current vs scan rate will be a linear function with the square root of the scan rate.[5]

Literature basis for the mechanism

Novoselsky and Menglisheva support our argument for adsorption of a species to the anode, and give some insight as to the species present.[7] Although the experiment described in their article utilizes a Co electrode, it outlines the possible oxidation pathway to CoOOH. The article suggests the mechanism shown in Eq. 1.4-1.8 for the oxidation of a Co electrode. Though CoO is our starting material that we use when creating our anode, it has been observed in our experiments and confirmed in the literature that Eq. 1.4 occurs spontaneously in alkaline solutions, therefore we use $Co(OH)_2$ as the starting material in our mechanism.[8]

$$CoO + H_2O \leftrightarrow Co(OH)_2 \quad 1.4$$

$$[CoOH]_{ads} + OH^- \leftrightarrow [Co(OH)_2]_{ads} + e^- \quad 1.5$$

$$[Co(OH)_2]_{ads} + 2OH^- \rightarrow [Co(OH)_4]^{2-}_{sol} \quad 1.6$$

$$[Co(OH)_2]_{ads} + OH^- \leftrightarrow [CoOOH]_{ads} + H_2O + e^- \quad 1.7$$

$$[CoOOH]_{ads} + OH^- \rightarrow [CoO_2]^-_{sol} + H_2O \quad 1.8$$

This mechanism is more comprehensive than the mechanism described by Eq. 1.1-1.3, and is more likely to better describe our electrochemical system.

Mechanism of global anodic reaction

In this section, I will describe each elementary step in greater detail, and outline the different theoretical pathways for the electroactive species. Because our experimental evidence suggests the oxidation of CoO to CoOOH contains both an adsorption and solution step, I will show these steps in the greater context of the overall mechanism.

The first step is the dissolution of CoO to $Co(OH)_2$, followed by the subsequent formation of complex ions in highly alkaline solutions.

$$CoO + H_2O \leftrightarrow Co(OH)_2 \quad 2.1$$

$$Co(OH)_2 + 2OH^- \leftrightarrow [Co(OH)_4]^{2-} \quad 2.2$$

Now dissolved in solution, the complex cobalt ion diffuses from the bulk solution to the electrode surface.

$$[Co(OH)_4]^{2-}_{bulk} \leftrightarrow [Co(OH)_4]^{2-}_{surface} \quad 2.3$$

Once at the surface, the electron transfer may take place by one of two reaction pathways. The first option requires that the electroactive species be dissolved, the reaction could either be quasi-reversible (2.4A) or irreversible (2.4B).

$$[Co(OH)_4]^{2-}_{surface} \underset{kc}{\overset{ka}{\rightleftarrows}} [CoOOH]_{ads} + H_2O + OH^- + e^- \quad 2.4A.$$

$$[Co(OH)_4]^{2-}_{surface} \xrightarrow{ka} [CoOOH]_{ads} + H_2O + OH^- + e^- \qquad 2.4B.$$

The second pathway is a reaction that occurs through a Co^{2+} intermediate which adsorbs in a separate step, and then becomes oxidized. The literature suggests this intermediate is $Co(OH)_2$, which would imply the following adsorption (2.5) and electron transfer (2.6) reactions.

$$[Co(OH)_4]^{2-}_{surface} \leftrightarrow [Co(OH)_2]_{ads} + 2OH^- \qquad 2.5A.$$

$$[Co(OH)_2]_{ads} \underset{kc}{\overset{ka}{\leftrightarrow}} [CoOOH]_{ads} + H^+ + e^- \qquad 2.6A.$$

Then, in our highly alkaline electrolyte (pH > 14), the proton produced from the oxidation reaction would very quickly react to form water.

$$H^+ + OH^- \rightarrow H_2O \qquad 2.7A.$$

However, we have not eliminated the possibility that $[Co(OH)_4]^{2-}$ is the adsorbed species, occurring by a similar pathway.

$$[Co(OH)_4]^{2-}_{surface} \leftrightarrow [Co(OH)_4]^{2-}_{ads} \qquad 2.5B.$$

$$[Co(OH)_4]^{2-}_{ads} \underset{kc}{\overset{ka}{\leftarrow\rightarrow}} [CoOOH]_{ads} + H_2O + OH^- + e^- \qquad 2.6B.$$

We believe that the global oxidation reaction involves a combination of the above reaction pathways. In all of these possible reaction mechanisms, the CoOOH product is adsorbed to the electrode, but we do not account for the passivation effect that decreases the current over time. This effect is beyond the scope of my thesis; as will be explained more completely later, our quantitative interpretation for the mechanism is based on a relatively clean electrode surface.

Kinetic models of electrochemical system used to interpret data from a chronoamperometry (a potential step) experimental technique and linear sweep cyclic voltammetry experiments.

We are pursuing a series of experiments with the goal of determining which reaction pathway outlined above best describes our observed electrochemical system. I will now outline the mathematical modeling that we used in order to find the best fit to our experimental data, assuming the electroactive species is in solution. As mentioned in the introduction, what follows is just an initial step in the modeling process.

For convenience, a short hand notation will be used to describe the mathematical development that follows: R is the reduced species in solution, $Co(OH)_2$ and the oxidized species O is CoOOH.

1-Dimensional mathematical model describing a chronoamperometry experiment when the reduced electro-active species is in solution:

$$R_{sol} \xrightarrow{ka1} O_{sol} + e^- \qquad 3.1$$

This model presumes that the electrochemical reaction is a one electron transfer completely irreversible reaction. It presumes that the only mode of mass transport is by Fickian diffusion, i.e. it excludes the possibility of forced convection. Furthermore, we presume a semi-infinite mass transfer boundary condition.

In a chronoamperometry experiment, the potential of the anode electrode with respect to the reference electrode is set to the open circuit potential, so that no current flows. After a delay of say some 15 seconds, the potential is stepped to a more positive value, thus initiating current flow. What follows is the mathematical model that describes how the current changes as a

function of time. The concentration of the electroactive species in this model is $C_R(x,t)$, at a given position from the anode surface at a given time.

The following partial differential equation (PDE) describes the situation where D_R is the diffusion coefficient of the reduced species.[9]

$$\frac{\partial C_R(x,t)}{\partial t} - D_R \frac{\partial^2 C_R(x,t)}{\partial x^2} = 0 \qquad 3.2$$

The initial condition is given by equation 3.3 and the boundary condition far from the electrode is given by 3.4.

$$C_R(x,0) = C_{R,bulk} \qquad 3.3$$

$$C_R(\infty,t) = C_{R,bulk} \qquad 3.4$$

The boundary condition at $x = 0$ is set by the chemistry of the electrochemical reaction. For the condition where we presume a one electron irreversible reaction at a high overpotential, the following equation applies:

$$D_R \frac{\partial C_R(0,t)}{\partial x} = k_{a1} * C_R(0,t) \qquad 3.5$$

Here, k_{a1} is the voltage dependent rate constant. The PDE with the corresponding initial and boundary conditions can be solved with Laplace transform techniques. The details for arriving at the solution are available in a number of texts.[5,10]

$$j = n * F * k_{a1} * C_R(0,t) * \exp\left[\frac{{k_{a1}}^2 * t}{D_R}\right] * \mathrm{erf}\left[\frac{k_{a1} * \sqrt{t}}{\sqrt{D_R}}\right] \qquad 3.6$$

This equation is useful for determining the D_R and k_{a1} for the electroactive species in solution, because it relates the current density (j) to the C_R, as well as Faraday's constant (F) and

the number of electrons transferred, which for this reaction is 1. The unknown parameters in equation 3.6 are established with a least squares nonlinear fit to the current vs. data from a chronoamperometry experiment. The code used to fit the data is given in Appendix (A-1).

1-Dimensional mathematical model describing a cyclic voltammetry experiment when both electro-active species are in solution:

We have also attempted using cyclic voltammetry to quantify the diffusion coefficient and the kinetic parameters of the reaction. Unlike chronoamperometry, this technique has a time dependent voltage input, complicating the mathematics considerably. But model equations 3.2-3.4 remain valid. What changes is the boundary condition at the electrode surface, $x = 0$. For example, if we presumed a reversible reaction that condition becomes the following time dependent form of the Nernst equation:

$$\frac{C_O(0,t)}{C_R(0,t)} = \exp\left[\frac{n*F}{R*T}\left(E - \nu t - E_f^o\right)\right] \qquad 3.7$$

Here, C_O is the concentration of the oxidized species (mol/cm^3), R is the universal gas constant (J/mol*K), T is temperature (K), E is the applied potential vs. the reference electrode (V), ν is the scan rate (V/s), and E^o_f is the formal potential of the electrochemical reaction (V).

The complexity of Eq. 3.7 does not change for an irreversible and a quasi-reversible boundary condition at the electrode surface. In short, this new boundary condition is not easily accommodated by Laplace transformation techniques. After applying Laplace transform techniques up to the electrode boundary condition, Randels and Sevcik back in the early part of the 20th century showed the concentration at the electrode in the Laplace domain is given by Eq. 3.8.[10]

$$\overline{C_R}(0,s) = \frac{C_{R,bulk}}{s} - \frac{j(s)}{F*D_R\left(\frac{s}{D_R}\right)^{\frac{1}{2}}} \qquad 3.8$$

In this equation, j(s) is the current density in the Laplace domain. The function is not known and finding it requires applying the boundary condition at the electrode. Randels and Sevcick do so, but in the time domain.

The inverse Laplace of this function is done with the convolution theorem, recognizing that

$$f(t) = \mathcal{L}^{-1}[j(s)] = j(t) \qquad 3.9$$

$$g(t) = \frac{1}{F*D_R} * \mathcal{L}^{-1}\left[\left(\frac{s}{D_R}\right)^{-\frac{1}{2}}\right] = \frac{1}{F*D_R} * \frac{1}{\sqrt{\pi*t}} \qquad 3.10$$

$$f(t) * g(t) = \int_0^\tau j(\tau)(t-\tau)^{-\frac{1}{2}}\, d\tau \qquad 3.11$$

$$C(0,t) = C_{R,bulk} - \frac{1}{F*\sqrt{D_R*\pi}} * \int_0^\tau j(\tau)(t-\tau)^{-\frac{1}{2}}\, d\tau \qquad 3.12$$

More mathematical work is required if one is to derive the function of current with respect to applied potential for the classic cases of a reversible, irreversible, and quasi reversible boundary condition at the electrode surface. But from an experimental point of view, one can work directly with the actual current vs. potential data. Using Eq. 3.12, a numerical integration is done to establish the values of the convolution integral as a function of time. We first convert current density to raw current (i) divided by the area (A).

$$C(0,t) = C_{R,bulk} - \frac{1}{F*A*\sqrt{D_R*\pi}} * \int_0^\tau i(\tau)(t-\tau)^{-\frac{1}{2}} * d\tau \qquad 3.13$$

Proceeding from here, we call I(t) the convoluted current and equate it to the integral in 3.13.

$$I(t) = \frac{1}{\sqrt{\pi}} * \int_0^{\tau} i(\tau)(t-\tau)^{-\frac{1}{2}} * d\tau \qquad 3.14$$

Then we find the limiting convoluted current $I_l(t)$ when $C_O(x,0)=0$ and $C_R(0,t)=0$ to calculate D_R, C_R and C_O.

$$I_l(t) = C_{R,bulk} * F * \sqrt{D_R} * A \qquad 3.15$$

$$C_R(0,t) = \frac{[I_l(t)-I(t)]}{F*A*\sqrt{D_R}} \qquad 3.16$$

$$C_O(0,t) = \frac{I(t)}{F*A*\sqrt{D_O}} \qquad 3.17$$

We obtain the limiting convoluted current by analyzing an experimental CV data file using a MATLAB code (Appendix A-2), which also calculates D_R, $C_O(0,t)$ and $C_R(0,t)$ over the anodic sweep of the CV. This code then outputs all these values into an Excel worksheet. This worksheet can be analyzed by another MATLAB code (Appendix A-3) in order to fit the data to the Butler-Volmer model for electron transfer kinetics, shown below.

$$i = F * A * k^o * \begin{Bmatrix} C_R * \exp\left[\alpha * \frac{F}{R*T} * \left(E - E_f^o\right)\right] - \cdots \\ C_O * \exp\left[-(1-\alpha) * \frac{F}{R*T} * \left(E - E_f^o\right)\right] \end{Bmatrix} \qquad 3.18$$

In this equation, k^o is the standard rate constant for the electron transfer step (cm/s) and α is the charge transfer coefficient (unitless). The parameters k^o, α, and E^o_f are calculated by the MATLAB code through a non-linear regression, and are used to generate a plot in order to evaluate the goodness of fit to the experimental data.

Discussion of results: determination of reaction mechanism

Identification of the electroactive species and products of the reaction

An additional goal of this research group is to quantify the current efficiency of the electrolysis process via bulk electrolysis. While that goal is not the main focus of this honors project, those experiments have provided us with key information as to the species present in the reaction.

The bulk electrolysis cell, a diagram of which is shown in Fig. 5, consists of a glass beaker containing KOH in a density gradient, with 40 wt% KOH on the bottom and 25 wt% KOH layered on top. The anode is made of multiple Ni foils with ~1.5 g CoO sandwiched between the foils. The cathode consists of multiple Pt foils. The beaker is then placed into a hot water bath and heated to 55 ^{o}C. The top of the beaker is sealed with a stopper containing outlet lines when quantifying the H_2 gas produced, but this seal can be removed when the goal is to quantify the solid products.

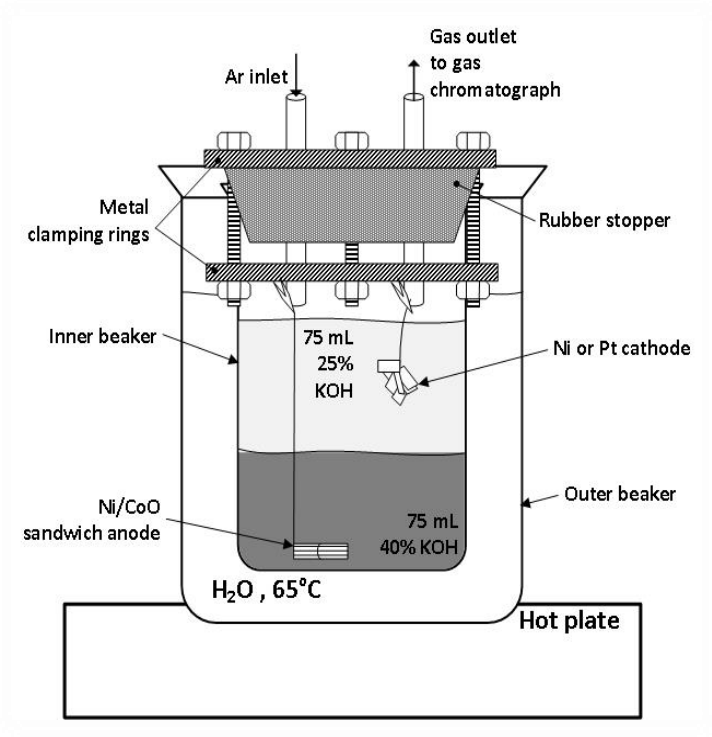

Figure 5. Complete electrolytic cell for quantifying current efficiency.

The electrolysis is performed at a potential between 1.0—1.3 V, generally starting at 1.2 V and increasing to 1.3 V when the current drops from electrode passivation. The electrolysis is generally stopped after about 1000 C have passed, corresponding to a little over 50% conversion to products. The solid mass is filtered, dried in an oven at 100 ^{o}C, then the mass is measured. The dried powder is then analyzed by x-ray diffraction (XRD) to determine the species present, and the XRD pattern is analyzed by Rietveld refinement to determine the relative amounts present.[11] Fig. 6 shows a typical XRD pattern with the peaks labeled with their respective species.

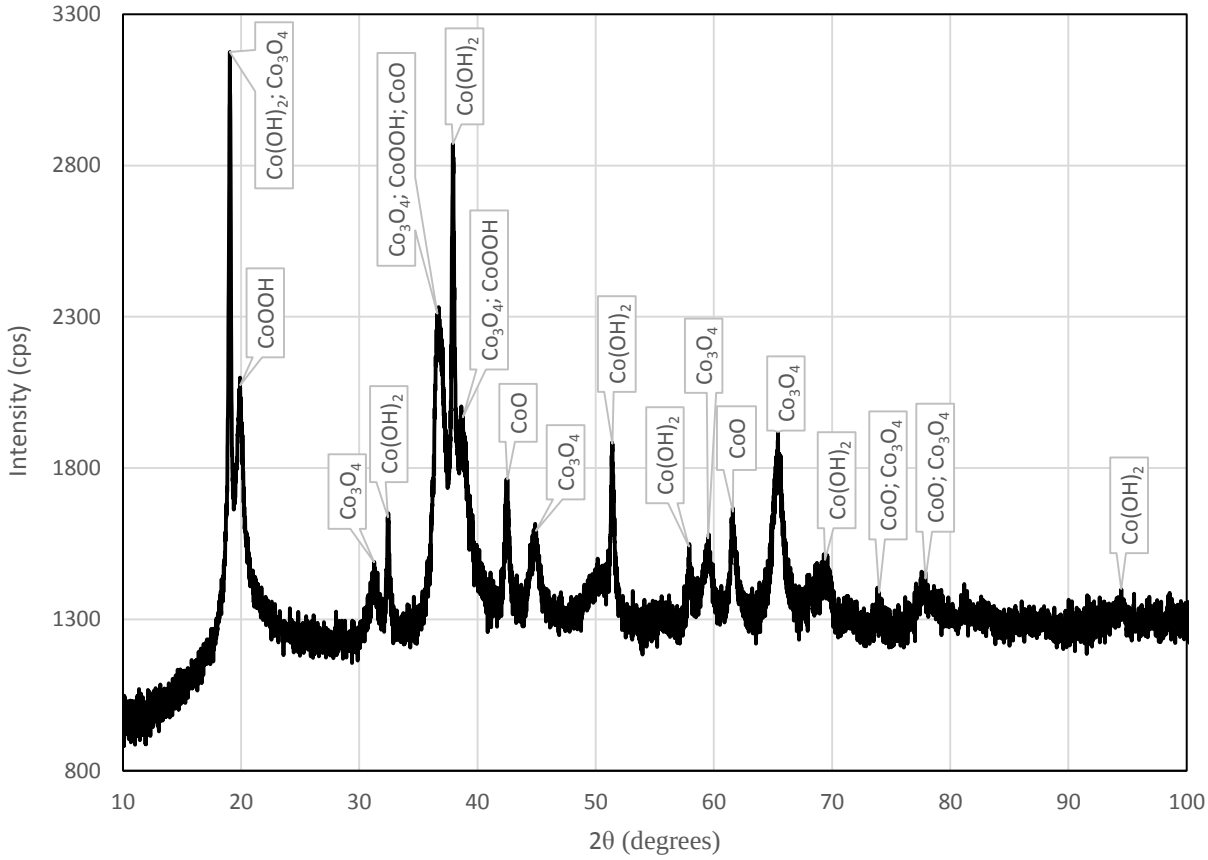

Figure 6. XRD pattern of post-electrolysis solid products.

From this information, we are confident that we have identified the species present in the electrochemical system. CoO is the starting material, and is converted spontaneously to $Co(OH)_2$ in the alkaline solution. After this, the $Co(OH)_2$ is electrolyzed to produce CoOOH and Co_3O_4.

We also needed to confirm that our voltammetric studies were investigating the same reaction as these bulk electrolysis experiments, the oxidation of Co^{2+} to Co^{3+}. To accomplish this, we connected an Ag/AgCl reference electrode to measure the potential of the anode and a multimeter to measure the cell potential. We then performed a potential sweep with respect to the reference electrode. This allowed us to plot the cell potential against the anode potential with respect to the reference electrode, the result of which is shown in Fig. 7. It can be seen that for the cell potential interval of 1.2—1.4 V, the potential with respect to the reference electrode

ranges between -0.058 and 0.024 V, in which we have observed the occurrence of the anodic oxidation peak. Thus, we confirmed that our voltammetry experiments are in agreement with our bulk electrolysis experiments.

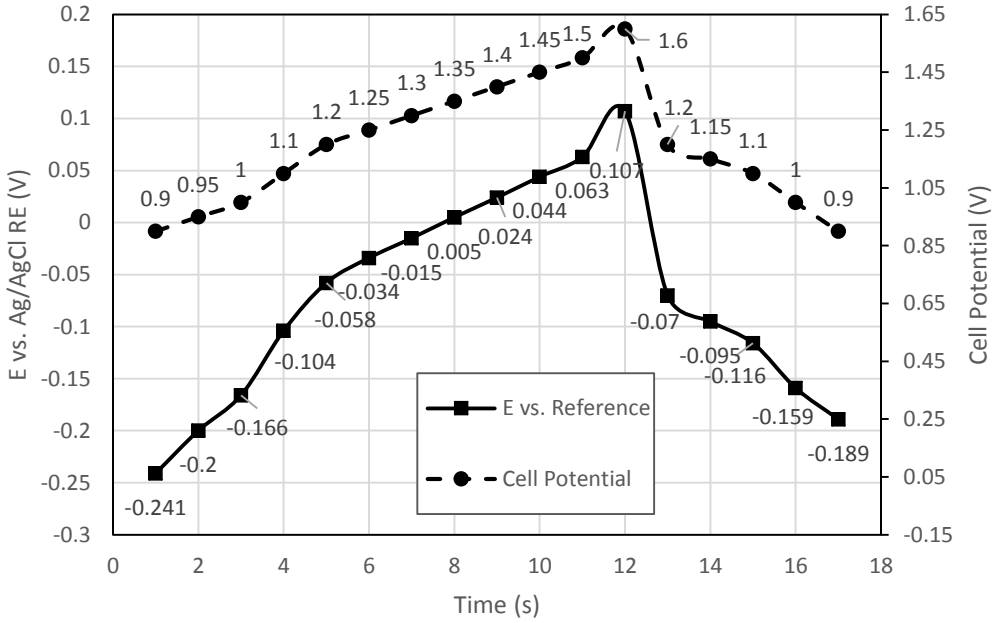

Figure 7. Cell potential and potential vs. reference electrode.

Evidence for adsorption of $Co(OH_2)$

The majority of the electrochemical data obtained to support the mechanism was done through voltammetry experiments. These experiments used a different electrochemical cell than the bulk electrolysis described above. The voltammetric cell, shown in Fig. 8, consisted of a small beaker containing 40 wt% KOH solution. The anode was made of two small Pt foils with $Co(OH)_2$ powder sandwiched in between. The cathode consisted of a set of Pt foils of area large enough to not limit the electron transfer process. The reference electrode was Ag/AgCl.

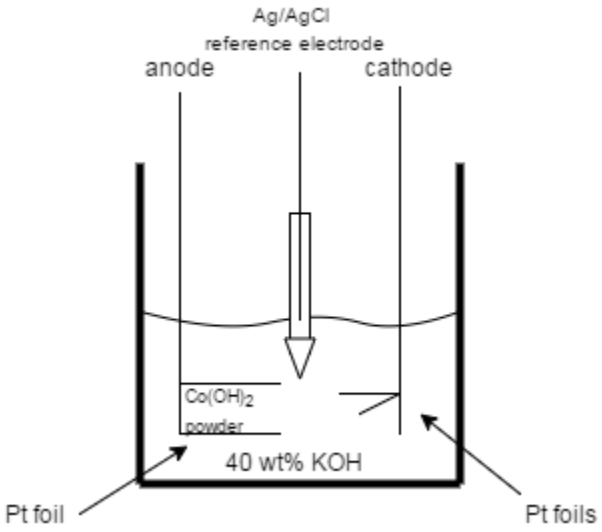

Figure 8. Electrochemical cell used in voltammetry experiments.

The possibility of $Co(OH)_2$ adsorption was initially considered because the shapes of the peaks in the CVs suggested this. Fig. 9 shows a CV with a symmetrical cathodic peak. This cathodic reaction could correspond to Eq. 5, with adsorbed $Co(OH)_2$ becoming reduced to CoOH. In addition, the anodic peak, visible in Fig. 10, has a somewhat symmetrical shape. This was difficult to confirm because the oxygen evolution reaction occurs before the current could return to zero or level off to a positive value.

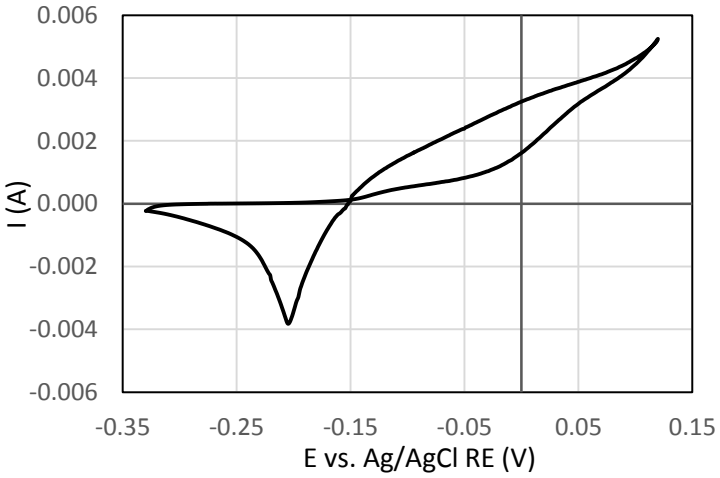

Figure 9. CV showing a symmetrical cathodic peak.

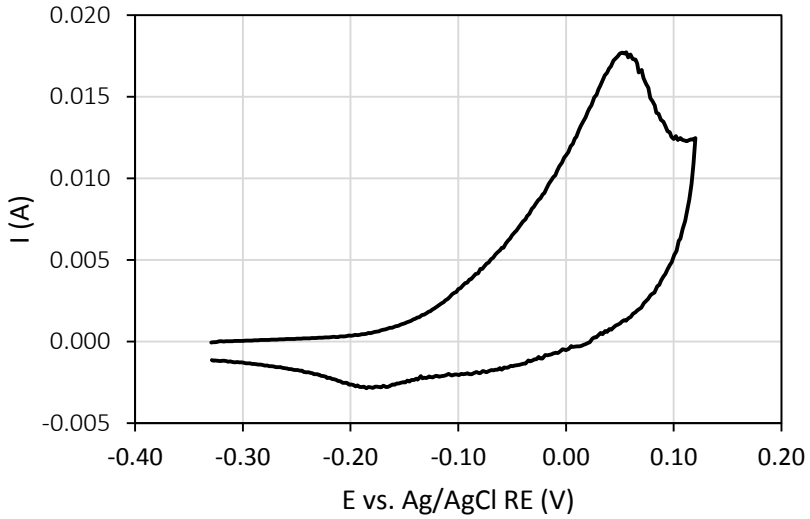

Figure 10. CV showing the ambiguous anodic peak.

We can use quantitative data from the CVs to clarify the nature of the reactions. A diagnostic test can be performed on a CV peak to determine if it corresponds to an adsorption or a diffusion process.[5] Setting the y-intercept of each trend line to zero, if the peak current varies linearly with the scan rate, the reaction is an adsorption process; if the peak current varies linearly with the square root of the scan rate, the reaction is diffusion-controlled. Fig. 11 is a CV that is representative of the CVs used for this diagnostic test.

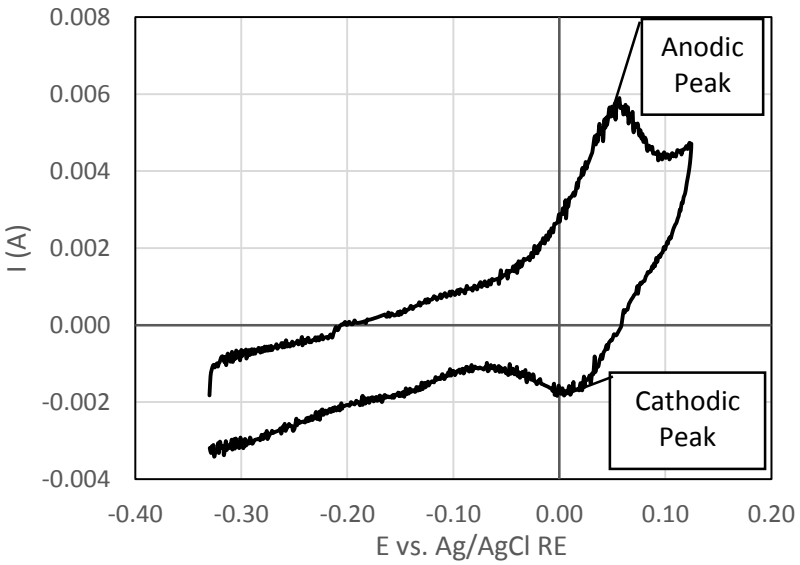

Figure 11. Typical CV shape used for Ip vs. v analysis.

This test was applied to the anodic peak and the cathodic peak in 14 CVs with scan rates ranging from 5—70 mV/s. It can be seen from Fig. 12 and 13 that the anodic peak current correlates more strongly to the square root of the scan rate rather than the scan rate directly, suggesting that this reaction is diffusion controlled. However, the cathodic peak has a stronger correlation to the scan rate directly than the square root of the scan rate, suggesting that this reaction is an adsorption process.

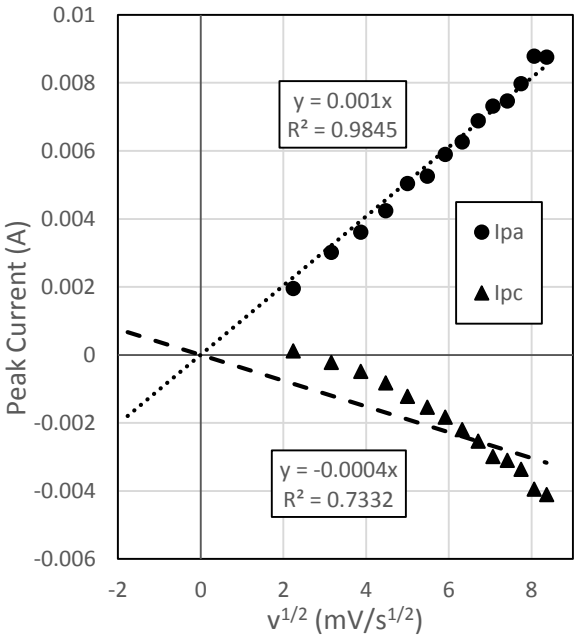

Figure 12. Diagnostic test for a diffusion controlled reaction for the large anodic peak and the cathodic peak.

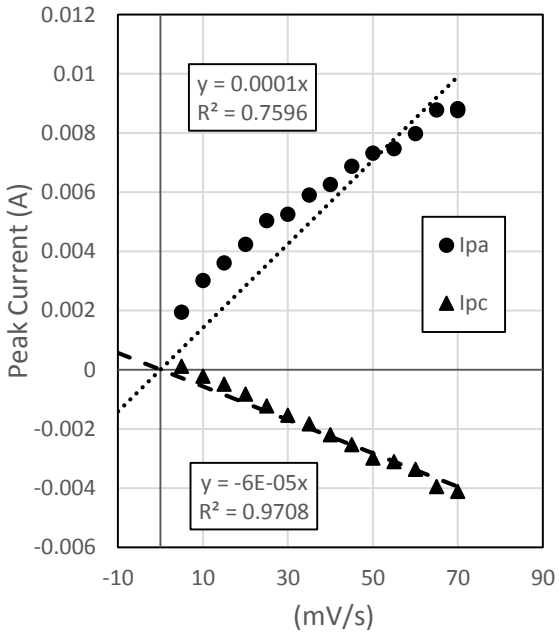

Figure 13. Diagnostic test for adsorption reaction for the large anodic peak and the cathodic peak

In short, we have evidence for an electrochemical process that involves both a solution reaction and an adsorption reaction. In this particular case, the mass transfer step seems to be more responsible for the anodic current than the adsorption reaction. But the reverse reduction scan suggests that at least some electroactive species in the anodic direction was adsorbed on the electrode.

Evidence for adsorption of $CoOOH/Co_3O_4$

Our mechanism also indicates that the product of the oxidation reaction, CoOOH are adsorbed to the surface. I will now show that we have evidence supporting this claim resulting from another type of electrochemical experiment called chronocoulometry.

A chronocoulometry response measures the charge passed after a step potential is applied to the electrochemical system. Charge is passed during electrolysis of the adsorbed and solution species and capacitive charging of the double layer of ions around the electrode[12]. The test for adsorption requires two potential step inputs, one above the oxidation potential and one below the reduction potential. Fig. 14 shows a two-step chronocoulometry response[12]. Here, the second potential step is applied at t = 100 ms.

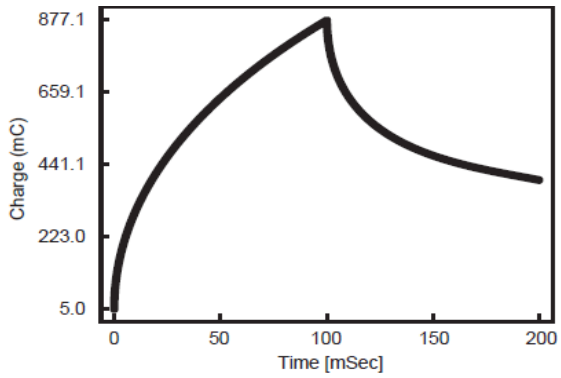

Figure 14. Sample two-step chronocoulometry response.

The two responses are separated, and the charge of the second step is shifted so that both step potentials are initially set to zero. The charge is then plotted against the square root of time. Fig. 15 shows a plot of this type from data obtained on our electrochemical cell. Before the first potential step, the electrodes are polarized at 0.125 V to electrolyze $Co(OH)_2$ and adsorb CoOOH to the anode. The first step drops the potential to -0.33 V to charge the double layer and reduce the CoOOH adsorbed during the pre-step, and the second step increases the potential back up to 0.125 V to charge the double layer.

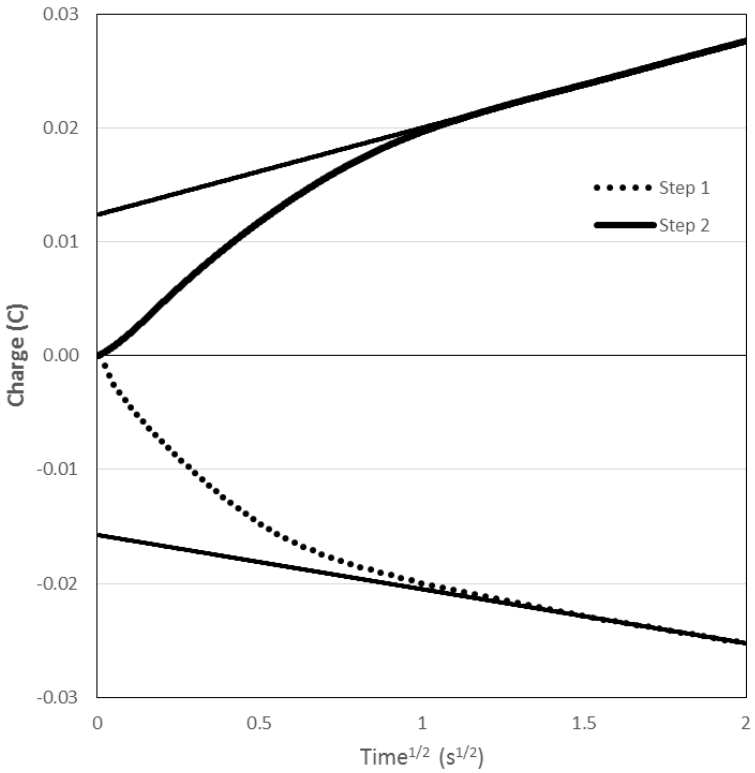

Figure 15. Chronocoulometry response: Pre-step = 0.125 V vs. Ag/AgCl Reference, 1 s. Step 1 = -0.33 V, 4 s. Step 2 = 0.125 V, 4 s.

Because the double layer charging and the electrolysis of the adsorbed species are nearly instantaneous, charged passed after this time is due only to electrolysis of the solution species. The linear portion of the curve arises because the electrolysis of solution species is diffusion controlled, so the current is constant. Extrapolating backward from this linear region gives the instantaneous charge passed immediately after each potential step is applied.

The magnitude of the slope of this region for the forward and backward steps are comparable, but the magnitudes of the y-intercepts are different. The y-intercept is about -15.9 mC for the forward step, and +12.5 mC for the reverse step. The charge from the forward step is due to the electrolysis of the adsorbed species and the charging of the double layer, while the charge from the backward step is due to only the charging of the double layer because there is no adsorbed species to electrolyze. Taking the difference between the magnitudes of these values

subtracts the charge from capacitance, leaving the charge from adsorbed species. For this potential step, the charge passed from electrolysis of CoOOH is 3.4 mC. I now move to show evidence of the two oxidation reactions occurring in parallel.

Evidence for parallel solution/adsorption oxidation reactions

We performed two experiments to understand further the oxidation pathway of Co metal to the Co^{3+} oxidation state, making small modifications to the electrolytic cell shown in Fig. 8. The Pt sandwich anode was replaced with a Co wire electrode and Ar was used to sparge the KOH prior to and during the experiment to remove dissolved oxygen from the solution.

In one experiment, the KOH electrolyte was saturated with $Co(OH)_2$ before performing electrolysis; in another experiment, there was no $Co(OH)_2$ dissolved. The type of voltammetric methods and the order that they were performed were identical in both experiments, in order to control the type of surface present on the anode.

The two cells behaved in similar ways. Fig. 14 shows a CV scan that encompasses all three electrochemical oxidations of the Co wire. We were most interested in the peak near -0.10 V, as we believe it to be the oxidation of Co^{2+} to Co^{3+}.

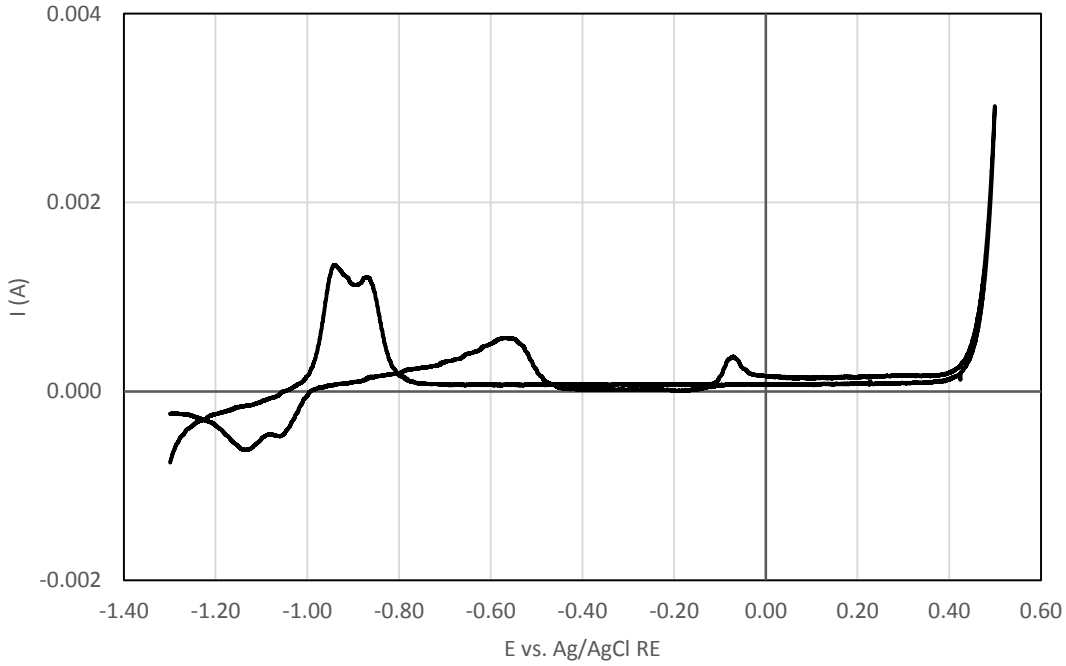

Figure 14. CV scan of Co wire anode depicting oxidation sequence of Co to Co^{3+}.

We focused CV scans to cycle around this oxidation peak several times, with interesting results. Fig. 15 and 16 show the CV scans around this peak for each cell.

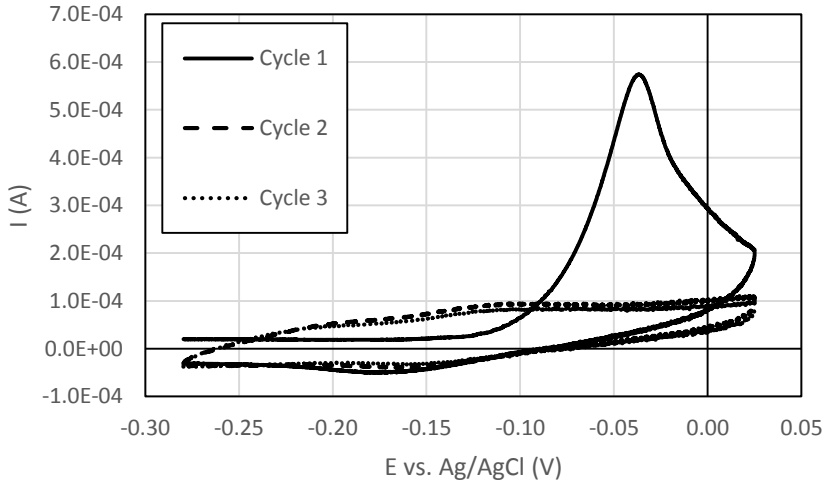

Figure 15. CV of CoOOH formation peak without $Co(OH)_2$ dissolved

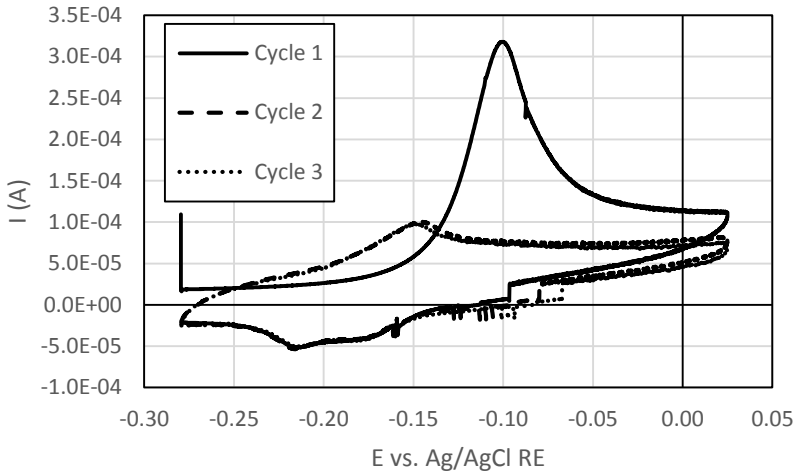

Figure 16. CV of CoOOH formation peak with $Co(OH)_2$ dissolved

It can be seen that the dissolved $Co(OH)_2$ has an interesting effect on the behavior of the cell. When $Co(OH)_2$ is not dissolved in the electrolyte, the second and third cycles of the CV pass minimal current, suggesting that the reaction does not occur on subsequent cycles. When $Co(OH)_2$ is dissolved in the electrolyte, the second and third cycles of the CV do indicate a small peak, suggesting that the oxidation reaction does occur.

The Ip vs. v diagnostic test was applied to this peak for all three cycles using scan rates of 5, 10, 20, and 30 mV/s for cycle 1, and scan rates of 5, 10, and 20 for cycles 2 and 3 because a peak current value was unidentifiable. These tests are shown in Fig. 17 and 18 and it can be seen that the anodic peak corresponds more strongly to an adsorption reaction than a solution reaction on all three cycles.

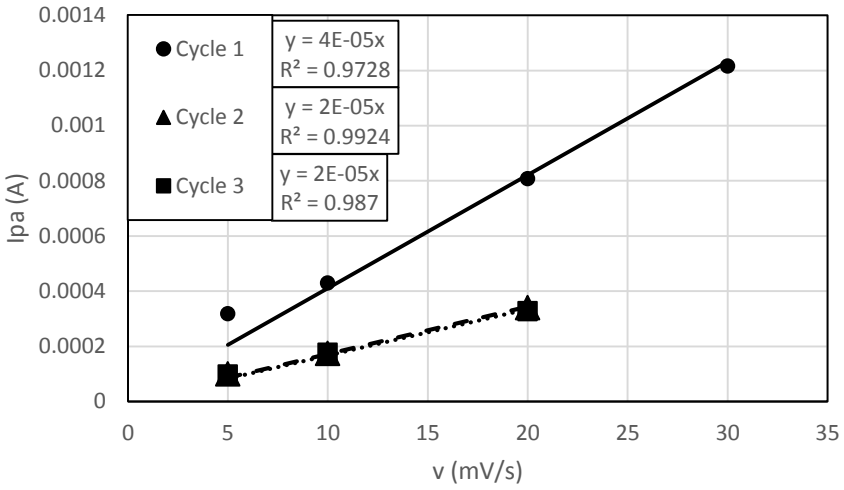

Figure 17. Diagnostic test for an adsorption reaction on anodic peak.

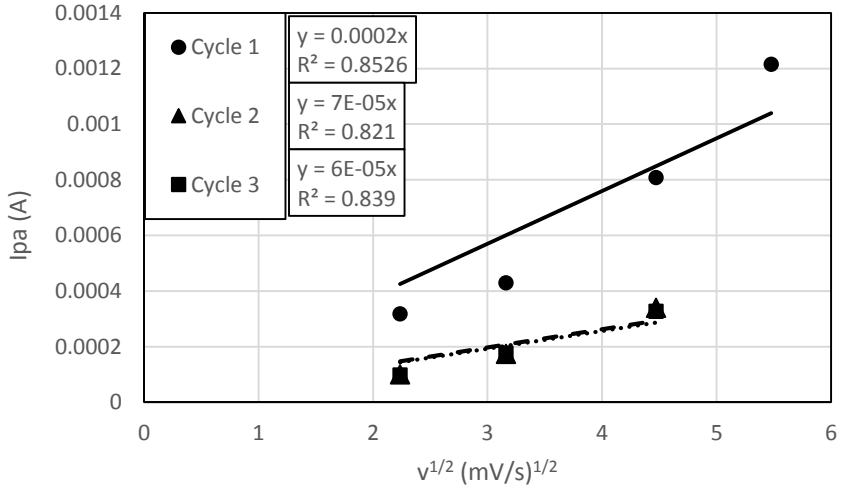

Figure 18. Diagnostic test for a solution reaction on anodic peak

From this information we draw the following conclusions: the dissolved $Co(OH)_2$ allows the oxidation reaction to occur on the second and third cycles because it adsorbs to the anode during the CV scan. The fact that the peak current is the same for the second and third cycles suggests that there is a limit to how much dissolved $Co(OH)_2$ can adsorb during the CV.

One might argue that the shapes of the CVs contrast with the conclusions drawn from the diagnostic test. The current does not drop to zero, as would be expected for an adsorption reaction. Additionally, the current remains constant for much longer than could be justified by the onset of the oxygen evolution reaction. Therefore, we propose that both the adsorption reaction and the solution reaction occur, but for the Co anode, they do so at similar enough potentials that they cannot be distinguished from each other on the CV. I will now show that this is supported by another set of CV data obtained using the Pt sandwich electrode and with some theoretical information.

When both the adsorbed species and the dissolved species are electrochemically active. Each species will undergo electrolysis, but at different voltages, and as a result two peaks will emerge in the CV. The location of the adsorption peak in relation to the solution peak is dependent on the stability of the species: For an anodic scan, if the reactant is adsorbed it will be more stable than that of the electroactive species in solution, thus one would expect the current peak at more positive potentials than for an electroactive species in solution. If the product is stabilized by adsorption, then the reaction peak occurs at a lower potential than the dissolved species reaction.[5]

This double-peak behavior is depicted in Fig. 19: a small peak or shoulder can be seen observed at approximately -0.14 V before the larger peak occurs near -0.06 V.

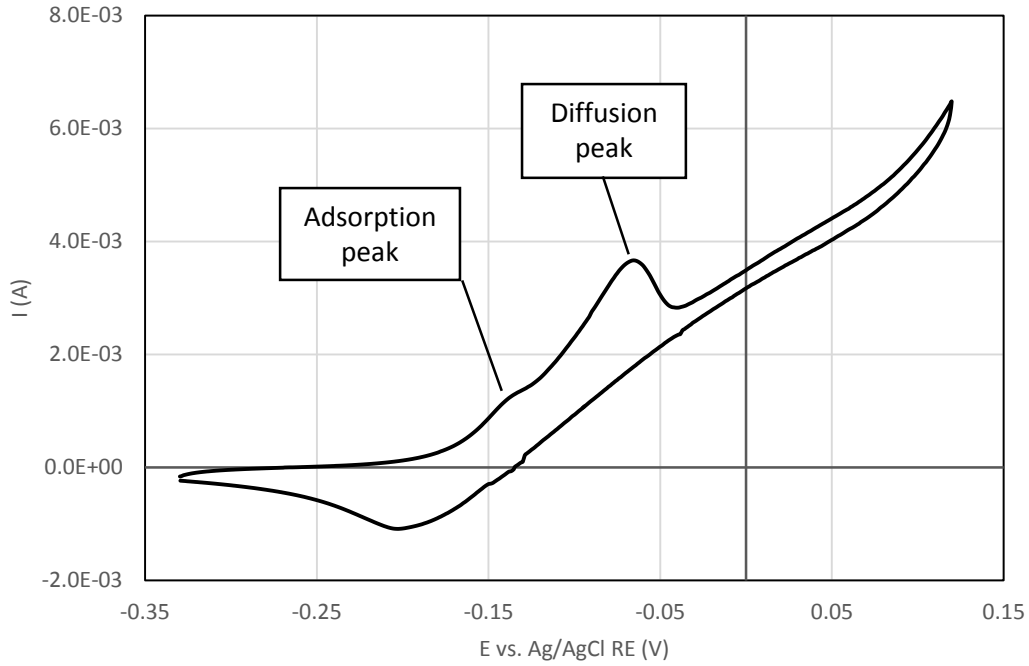

Figure 19. Cyclic voltammetry scan: 1 mV/s scan rate, -0.33 to 0.12 V vs, Eref

If the larger peak corresponds to the solution reaction, as suggested by the diagnostic tests in Fig. 12 and 13, then the smaller peak would correspond to the adsorption reaction. In highly alkaline solutions, $Co(OH)_2$ accepts extra OH^- ions to form $Co(OH)_4^{2-}$. For this dissolved species, the oxidation reaction could be occuring as shown below.

$$Co(OH)_4^{2-} \rightarrow CoOOH + H_2O + OH^- + e^-$$

The pre-peak could be the reaction in Eq. 1.7 occurring, as CoOOH is observed as a product and the chronocoulometry data suggest it is adsorbed. The theoretical background of the coordination states of Co also supports the stability of the adsorbed species.

As mentioned before, $Co(OH)_2$ will convert to $Co(OH)_4^{2-}$ in alkaline solutions. This ion will likely have a tetrahedral geometry when free in solution. When the ion adsorbs to the Ni surface, a conformational change will occur in order to account for the additional ligand. Two

options are available for the new geometry, trigonal bipyramidal and octahedral. The octahedral geometry will cause the Co ion coordinate to a water molecule in either an axial or equatorial position. Fig. 20-23 show the different possible geometries of the $Co(OH)_4^{2-}$ ion in solution and after adsorption.

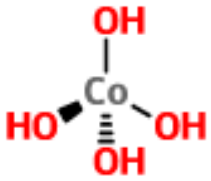

Figure 20. Tetrahedral geometry of dissolved $Co(OH)_4^{2-}$.

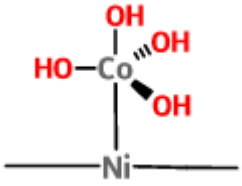

Figure 21. Trigonal bipyramidal geometry of adsorbed $Co(OH)_4^{2-}$.

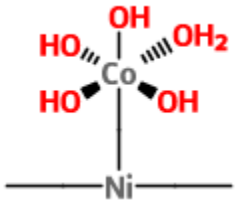

Figure 22. Octahdral geometry of adsorbed $[Co(OH)_4^{2-}]H_2O$, equatorial H_2O

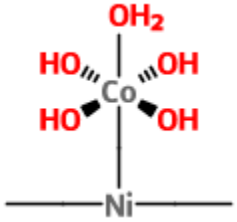

Figure 23. Octahedral geometry of adsorbed $[Co(OH)_4^{2-}]H_2O$, axial H_2O.

The different geometries have different stabilities, based on the coordination state of the Co ion and the ligands. Once the Co^{2+} ion adsorbs to the Ni surface with its OH^- ligands, it is energetically favorable for it to adopt an octahedral geometry and undergo oxidation to Co^{3+}. This satisfies the 18 electron rule for transition metals, which arises from the stabilization effect of filling the 9 bonding and nonbonding molecular orbitals created by the metal and its ligands.[13] The electron count for this coordination complex is as follows: Co^{2+} has 7 valence electrons, 2 electrons are donated by the H_2O ligand, 2 x 4 electrons are donated by the OH^- ligands, and 2 electrons in the Ni-Co bond total 19 electrons in the complex. By losing one electron through oxidation, the complex will now have 18 electrons, gaining the maximum stabilization effect.

Thus our proposed explanation of the two peak locations is supported by this theoretical information.

Discussion of results: quantitative evaluation with mathematical models

Our plan for confirming the reaction mechanism as a combination of the steps described in the theoretical section requires an understanding of the extent to which each pathway contributes to the overall reaction. We suspect that one pathway may occur with faster reaction kinetics, with the other acting as a rate determining step. Thus, we have attempted to devise experiments that examine the adsorption reaction separately from the solution reaction. In these experiments, we seek to establish a condition so that one reaction predominates over the other.

In order to elucidate the behavior of the adsorption reaction, it is imperative that we obtain a repeatable result. This is complicated by the fact that each electrochemical process we perform changes the surface of the electrode. Thus, our first task was to establish a procedure for restoring the electrode surface, so that each electrochemical measurement can be made under similar conditions.

We examined cyclic voltammograms of the Co wire and noted the potentials that each oxidation reaction occurred, in order to use them in our resurfacing procedure. We applied the first potential step at -1.3 V vs. Ag/AgCl for 120 seconds; the negative current of this step indicated that the electroactive material was being reduced, likely back to Co. Then, we applied a second potential step at -0.6 V vs. Ag/AgCl for 120-240 seconds to oxidize the electrode surface to $Co(OH)_2$, seeking a final current near 40 μA. Thus, with this conditioning, we assumed the surface composition to be mostly $Co(OH)_2$.

We applied this preconditioning process to a Co electrode in 40 wt% KOH (A = 0.366 cm^2) with no dissolved $Co(OH)_2$ particles to force the dominance of the adsorption reaction. While we understand that the $Co(OH)_2$ on the electrode surface may dissolve into the solution, we assume this dissolution to be minimal and that the adsorption reaction occurs much more readily.

There are a myriad of electrochemical techniques, based on all the different principles of electrochemistry, each capable of determining certain characteristics of the electrochemical system in some way. It is often helpful to group them according to the type of environment they create during the course of operation: they can force an altered, but stable profile, or they can elicit a non-steady response.

The former includes the convection produced by a rotating disc electrode, or the measured response from an alternating current signal of electrochemical impedance spectroscopy. Both of these have possible futures with this project. In the present however, we have at our disposal a technique that requires no special equipment, or no deep technical understanding of complex electronic principles.

The Tafel approximation, as it is called, is a modification of Eq. 3.18, the relationship between current density and the kinetic parameters. This manipulation can be applied to any data measured by a non-steady method as there exists a region where the overpotential $E - E^o_f$ or also called η, is high enough that one exponential term of Eq. 3.18 becomes minimal. For the anodic case, our half-reaction of interest, the more positive overpotential decreases the right term of Eq. 3.18 to zero. This alters the current density plot so that the following is true.

$$j = F * k^o * C_R * \exp\left[\frac{\alpha * F * \eta}{R * T}\right] \qquad 4.1$$

There is an important assumption: $C_R = C_R^{bulk,}$ a. In other words we have a large enough overpotential to avoid the back reaction, but not so large that there is a substantial drop in the concentration of the electroactive species at the electrode. The analysis then utilizes the values of C_R^{bulk} from literature and the temperature of the cell.[8] We express equation 4.1 in terms of the exchange current density (j_o), a fundamental constant related to the rate of the electron transfer in the both the anodic and cathodic directions. After this, the following plot can be made by taking the natural log of each side. This allows us to determine j_o and α.

$$\ln(j) = \frac{\alpha * F}{R * T} * \eta + \ln(j_o) \qquad 4.2$$

This analysis is shown below in Fig. 24, where the linear region is shown laid over the current from a larger potential range. From this plot, we calculated a j_o = 2.4E-4 A/cm^2 and α = 1.2. The results from the all CVs analyzed in this fashion are shown in Table 1.

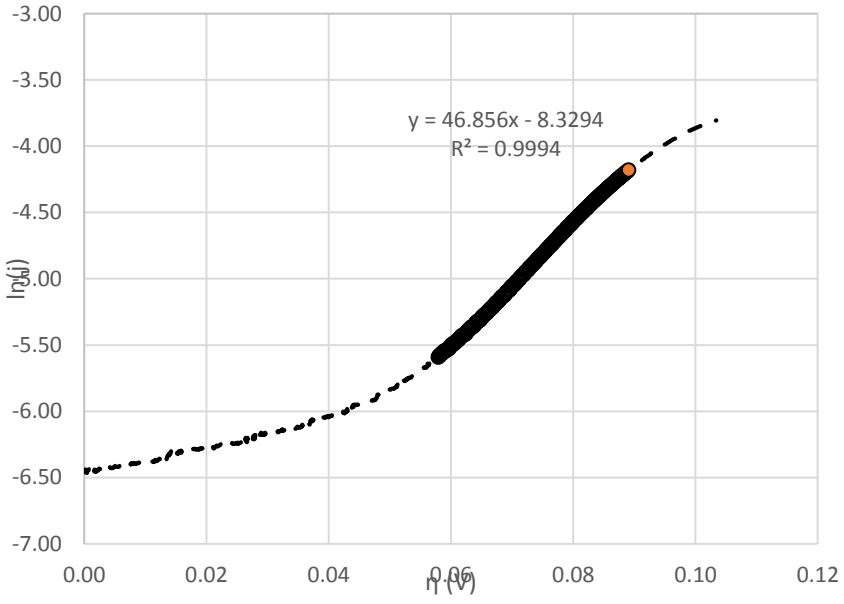

Figure 24. Tafel approximation of a CV with a 60 mV/s scan rate

ν (mV/s)	j_o (A/cm^2)	α
10	2.5E-4	0.66
20	4.5E-4	1.4
30	3.9E-4	1.4
40	4.4E-4	1.2
50	2.3E-4	1.3
60	2.4E-4	1.2

Table 1. Kinetic parameters determined by Tafel approximation

The exchange current density values seem to stay within a reasonable range. However, because α does not hold a value between 0 and 1, it means that this Tafel approximation of Eq. 3.18 does not completely describe the current density, and we hope that modeling the adsorption step will correct for this. Additionally, the Tafel approximation is better at slower scan rates, and because the 10 mV/s CV returned reasonable values of j_o and α, we plan to repeat this analysis for CVs performed between 1-10 mV/s.

Conversely to the steady state techniques exist the non-steady state techniques, which for us include chronoamperometry and cyclic voltammetry.

We can use chronoamperometry to determine k^o and D_R as well by using the model derived in the theoretical section, ending with Eq. 3.6, making the assumption that the concentration that the $C_R(0,t) = 0$ at a high anodic overpotential.

Using a custom MATLAB code (Appendix A-1), we can use regression tools to fit the data we obtain in our experiments to Eq. 3.6. This curve fitting will determine the diffusion coefficient as well as k_{a1} (reported as k_f in the output) of the anodic oxidation reaction. We have obtained a result for one chronoamperometry response at the time of writing, shown in Fig. 25 with the calculated parameter values.

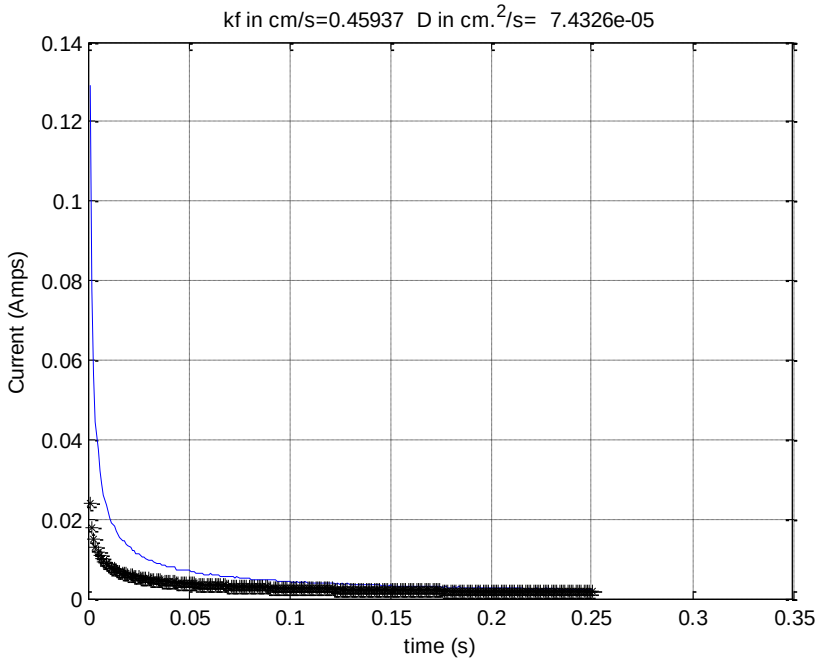

Figure 25. Curve fit (* markers) of data from 3/23/16 experiment (solid line), -0.07 V vs. Ag/AgCl applied potential.

The calculated model fits the data better after about 0.1 s than it does immediately after the potential step is applied. Our current explanation for this is that we have not included any effect of the adsorption step of the reaction mechanism into this model yet.

We have also evaluated the model using cyclic voltammetry, the other non-steady state technique. We performed cyclic voltammetry scans at scan rates from 10-60 mV/s in 10 mV/s intervals, performing the resurfacing method in between each cyclic voltammogram. We then used the two MATLAB codes to analyze the cyclic voltammetry files in order to determine the parameters D_R, α, k^o, and E^o_f, as well as to curve fit the calculated model to the data.

The curve fit output of this program for the CV obtained at 50 mV/s is shown below in Fig. 26. The calculated values for each scan rate are shown in Table 2.

ν (mV/s)	D_R (cm^2/s)	k^o (cm/s)	α	E^o_f (V)
10	4.4E-4	7.4E-6	0.54	-0.29
20	6.9E-4	1.2E-5	0.59	-0.28
30	8.6E-4	4.1E-6	1	0
40	1.1E-3	9.8E-6	0.47	-0.26
50	1.4E-3	5.9E-6	0.46	-0.28
60	1.7E-3	2.0E-6	0.41	-0.31

Table 2. Calculated kinetic parameters for CVs obtained on 3/23/16

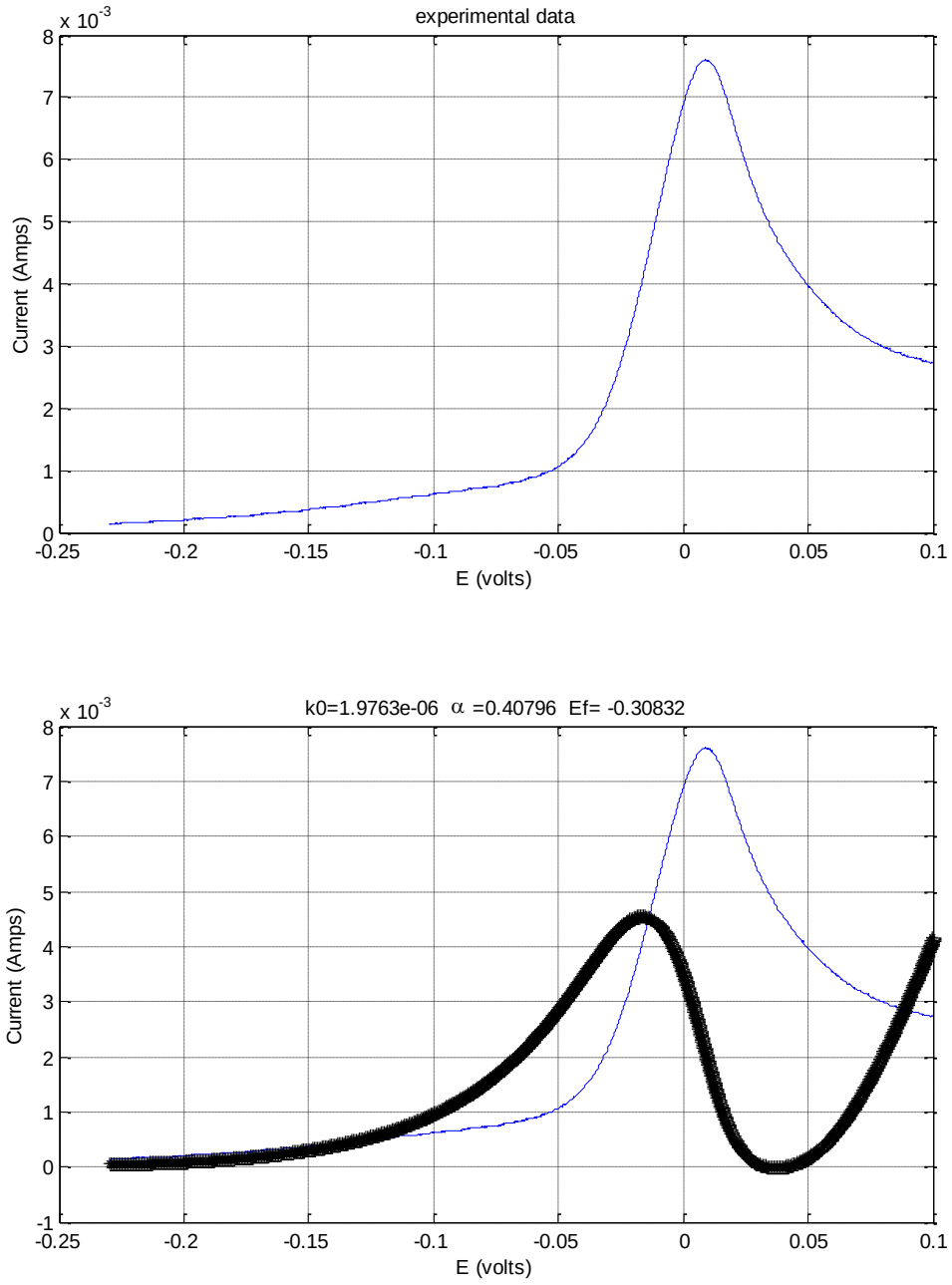

Figure 26. Output of MATLAB code from 3/23/16 experiment. Top: Experimental data analyzed by code. Bottom: Curve fit (+ markers) of experimental data (solid line).

It is clear that we do not have an acceptable quantitative description of the electrochemical processes. Firstly the diffusion coefficients between the CA and CV experiments differ beyond an acceptable amount. Secondly, the regression analysis of the CV data gives a

very poor fit. On the positive side of the result, we can say that this mathematical result demonstrates that the electrode process is more complex than that of an electron transfer step to an electroactive species in solution.

Also, it is appropriate to say that the model, although not adequate, represents a first step at developing one that accounts for adsorption.

Future work

These experiments and analyses conclude my honors thesis within this project. However, the future of the project includes more work to develop the kinetic model to obtain a more complete picture of the electrochemical system. Our mathematical model currently does not include the adsorption step of the reaction, which we have confirmed through our experimental evidence. A better model will account for this complexity, especially as we have described it occurring simultaneously with the electron transfer to species in solution. Once this is done and the MATLAB programs are altered accordingly, experiments can be performed and the data can be analyzed to obtain more reliable values of the kinetic parameters. Later, these parameters can be evaluated to determine the viability of scaling this process up to an industrial level.

Acknowledgements

I would like to acknowledge Dr. Robert Palumbo and Dr. Jonathan Schoer for their guidance and mentorship in the perplexing world of electrochemistry and thesis writing, Carol Larson and Daniel Kotfer for their help in performing the experimental procedures, Joshua Grade for his expertise in MATLAB coding, Evan Beyers and Jordan Otto for beginning the investigation of CoO, the Valparaiso University Scholarship and Advising Committee for allowing me to pursue this work, and the National Science Foundation for funding the project. I

would also like to thank my family and friends for supporting me in this challenging undertaking.

Bibliography

Cited

(1) Häussinger, P. ; Lohmüller, R. ; Watson, A. M. In *Ullmann's Encyclopedia of Industrial Chemistry*; Wiley-VCH Verlag GmbH & Co. KGaA: Weinheim, Germany, 2011.

(2) Splitting Water Offers an Inefficient but Effective Way to Store Energy | MIT Technology Review http://www. technologyreview. com/news/530331/germany-and-canada-are-building-water-splitters-to-store-renewable-energy/ (accessed Aug 12, 2015).

(3) Palumbo, R. ; Diver, R. B. ; Larson, C. ; Coker, E. . ; Miller, J. E. ; Guertin, J. ; Schoer, J. ; Meyer, M. ; Siegel, N. P. *Chem. Eng. Sci.* **2012**, *84*, 372–380.

(4) Elumalai, P. ; Vasan, H. N. ; Munichandraiah, N. *J. Power Sources* **2001**, *93* (1-2), 201–208.

(5) PLETCHER, D. ; GREFF, R. ; PEAT, R. ; PETER, L. M. ; ROBINSON, J. In *Instrumental Methods in Electrochemistry*; Elsevier, 2010; pp 178–228.

(6) Cyclic Voltammetry https://en. wikipedia. org/wiki/cyclic_voltammetry (accessed 2015).

(7) Novoselsky, I. M. ; Menglisheva, N. R. Electrochemica Acta 1983, 29 (1), 21-27.

(8) Ziemniak, S. E. ; Goyette, M. A. ; Combs, K. E. S. *Journal of Solution Chemistry* **1998**, *28* (7), 809-836.

(9) Fick, A. *Journal of Membrane Science* **1995**, *100* (1), 33.

(10) Bard, A. J. ; Faulkner, L. R. Electrochemical methods: fundamentals and applications; Wiley: New York, 1980.

(11) Rietveld, H. M. Journal of Applied Crystallography 1969, 2, 65.

(12) Bott, A. ; Heineman, W. *Current Separations* **2004**, *20* (4), 121-126.

(13) Miessler, G. L. ; Tarr, D. A. Inorganic chemistry, 4th ed. ; Pearson Prentice Hall: Upper Saddle River, N. J. , 2011.

Additional Readings

Gerken, J. B. ; McAlpin, J. G. ; Chen, J. Y. C. ; Rigsby, M. L. ; Casey, W. H. ; Britt, R. D. ; Stahl, S. S. *J. Am. Chem. Soc.* **2011**, *133* (36), 14431–14442.

Kabasakaloglu, M. *Turkish J. Chem.* **1994**, *18* (1), 41–50.

Kreysa, G. *Electrochim. Acta* **1988**, *33* (10), 1351–1357.

Pralong, V. ; Delahaye-Vidal, a. ; Beaudoin, B. ; Gérand, B. ; Tarascon, J. -M. *J. Mater. Chem.* **1999**, *9* (4), 955–960.

Appendix A-1: MATLAB code for analysis of chronoamperometry data

```
%This code gives current density vs time for an electrochemical system's
%anode experiencing a step change in potential vs a silver/silver chloride
%electrode. Furthermore it is presumed that the electrochemical reaction is
%the following: R(sol)------O(sol) + e. The only mode of mass transport is
%molecular diffusion.  It is a one dimensional model. The output is a
%voltage dependent rate constant and the Diffusion Coefficient of the
%electro-active species.


% _____________________________________________________________________________%
% Author                            Date                          Comments
% R. Palumbo                      March 2016                   Original Code
%_____________________________________________________________________________%



% Excel File Import:  Retrieving experimental data from an excel spread sheet
clear
Sheet_Name='CA_15';
Sheet_Page=2;
Sheet_Range='A6:B255';
Data_Exp=xlsread(Sheet_Name,Sheet_Page,Sheet_Range);
Time = Data_Exp(:,1);
Current= Data_Exp(:,2);
%plot(Time, Current)

ydata=Current;% [i]
xdata=Time;


%% CONSTANTS
     F=96485. 3365; % s A / mol
     R=8. 3144621; %J/mol-K
     T=295; % K
     A=0. 366; % cm^2 Anode Area
     f=F/(R*T);
     n= 1; %mole of electrons per mole of products
     CRb= 5e-6; %bulk concentration of Co(OH)2, mole/cm^3
%% CURVE_FIT SETUP
  options = optimoptions('lsqcurvefit');
  options. TolX = 1e-15;
  options. MaxIter = 10000;
  options. TolFun=1e-10;
  options. MaxFunEvals=10000;
  %options. Algorithm='levenberg-marquardt';
%% CURVE_FIT COMMAND
x = lsqcurvefit(@myfunCA,[. 1,. 1], xdata, ydata,[0,0],[inf,inf],options);
 %THE RESULTS

Y_Reg = CRb*n*F*A*x(1). *exp(x(1)^2. *xdata. /x(2)). *(erfc(x(1). *. . . . .
        (xdata). ^(. 5). /sqrt(x(2))));
   kf=x(1) % cm/s
```

```
   D= x(2) %cm^2/s



plot(xdata,ydata,xdata,Y_Reg,'*k')
%plot(xdata,Y_Reg)
%legend('Exp. ', 'Fitted Data')
xlabel('time (s)')
ylabel('Current (Amps)')
grid on

title (['kf in cm/s=',num2str(x(1)),' ' 'D in cm. ^2/s= ',num2str(x(2))])
```

Appendix A-2: MATLAB code for obtaining convoluted current from cyclic voltammetry data

```
%-------------------------------------------------------------------------%
%This code allows one to do a numerical convolution integral analysis of
%electrochemical data from a cyclic voltammetery experiment described
%as follows: O(sol) + e-----R(sol). The system is 1 Dim with one BC at
%x = inf, where the bulk concentrations of O and R are given.  All
%transport is by molecular diffusion.

%The program converts current vs time data into convoluted current vs time
%data.It leads directly to the concentration of the electroactive species at
%the electrode vs time. It also directly gives the diffusion coeff. of the
%electroactive species.  The concentration vs. time data can also be
%processed further with a non-linear regression routine to solve for kinetic
%parameters such as the specific rate constant or the exchange current
%density and the transfer coeff.  This second program is where the details
%of the boundary condition at the electrode are specified: quasi rev or
%IRR, etc.

%%%%%%%%%%%%%%%%%%%%%%%%%%%%%%%%%%%%%%%%%%%%%%%%%%%%%%%%%%%%%%%%%%%%%%%%
%Original Code                          S. Nudehi       Fall 2014
%Data processing Input/Output           J. Grade        Summer 2015
%Tweaking for ME 475                    R. Palumbo      Spring 2016
%%%%%%%%%%%%%%%%%%%%%%%%%%%%%%%%%%%%%%%%%%%%%%%%%%%%%%%%%%%%%%%%%%%%%%%%

%The code is written assuming that the data is from a reduction
%wave.  The negative currents are converted for convenience to positive
%values.  Some care is needed if one is to use the code for an oxidation
%wave.  The data: time, current, convoluted current, applied voltages, and
%the diffusion coefficient are all saved in an Excel spreadsheet in a form
%ready for am in-house nonlinear regression analysis program.


clear all;
close all;
clc;

%% INITIAL PARAMETERS specific to NSF includes Anode area and Cbulk for Dcalc
A =  .366;      % area of anode cm2
n =  1;         % electrons transferred
Cbulk = 5.1e-6; % bulk concentration must be in mole/cm^3
TOGGLE = 0;     % if 1, then averaging is enabled.  Most likely stays 0

%% READ EXCEL DATA

Book_Name='ME475 fast scans';
Sheet_Page=5;
Sheet_Range='C127:E6127'; %you want the CV data time, voltage and current
                          %you are using only the data from the reduction
                          %wave.  It may be helpful to start the data when
                          %the current is zero or just about to go
                          %negative. It should stop at the value of the
                          %switching potential where the oxidation wave
                          %begins.
```

```
Data_Exp=xlsread(Book_Name,Sheet_Page,Sheet_Range);
T = Data_Exp(:,1); %time vector
V = Data_Exp(:,2); %voltage vector
C = Data_Exp(:,3); %current vector

%% AVERAGE DATA POINTS

if TOGGLE == 1

    z = 1; x = 5; y = 1;
    for count = 1:length(C)/5
    a(count) = mean(C(z:x));%mean of the currents
    b(count) = mean(V(z:x));%mean of the voltage
        if y == 1;
            c(count) = T(y); %getting time of every 5th point
            y = y + 4;
        else
            c(count)=T(y);
            y = y + 5;
        end
    x = x + 5;
    z = z + 5;

    end
    Current_avg = a';
    Potential_avg = b';
    Time_corr = c';

else
    Time_corr = Data_Exp(:,1); %time vector
    Potential_avg = Data_Exp(:,2); %voltage vector
    Current_avg = -1* Data_Exp(:,3); %current vector multiplied by -1 so
                                     %that the negative current is made +
end

%% CONVOLUTION Based on Bard and Faulkner page 248-249 2nd edition
delta_t = abs(Time_corr(2)- Time_corr(1));
k_max = length(Time_corr);

n=1/delta_t;
for k = 1:(k_max-1),
      Inner_Sum=0;
  for j = 1:k,
Inner_Sum = Inner_Sum +1/sqrt(pi)*(Current_avg(j)+Current_avg(j+1))/2* ...
     sqrt(delta_t)/sqrt(k-j+1/2);
  end
      Conv_Current(k)=Inner_Sum;
end

Conv = [delta_t*[1:k_max-1]', Conv_Current(:)];
%% FIND D

D = ((max(Conv_Current))/(96485*A*Cbulk))^2;
```

```
disp('        Diffusion coefficient based on convolution:')
disp(['        ' num2str(D,'%5.3e') '  cm^2/s'])

%% FIND CR AND CO in mole/cm^2
Co = (max(Conv_Current)-Conv_Current)/(96485*A*sqrt(D)); %concentration of
                                                         %oxidized species
Cr = (Conv_Current/(96485*A*sqrt(D)))';%the number is the concentration of
reduced species
%% PLOT RESULTS
index = length(Current_avg) - 1;

set(gcf,'color','w')

subplot(2,2,1)
plot(Potential_avg,Current_avg)
title('Current vs. Potential')
xlabel('Potential [V]')
ylabel('Current [C/s]')

subplot(2,2,2)
plot(delta_t*([1:k_max-1]), Conv_Current)
title('Convoluted Current vs. Time')
xlabel('Time [s]')
ylabel('Convoluted Current [A/s^1/2^]')

subplot(2,2,3)
plot(Conv(:,1),Cr,'-k',Conv(:,1),Co,'-b')
title('Concentration vs Time')
xlabel('Time [s]')
ylabel('Concentration [mol/cm^3^]')
legend('Cr','Co','location','northwest')

subplot(2,2,4)
plot(Conv(:,1),Current_avg(1:index),'-b',Conv(:,1),Conv(:,2),'-k')
title('Current and Convoluted Current')
xlabel('Time [s]')
ylabel('Current [C/s]or A/s^1/2^]')
legend('Current','Conv','location','northwest')

% Outputing data to Excel Data sheet
    if TOGGLE == 1
    xlsfile = 'Convoluted_Current_Data_Averaged_RP.xlsx';
    Data = [Time_corr(1:index) Current_avg(1:index) Potential_avg(1:index)
Time_corr(1:index) Co Time_corr(1:index) Cr' Conv(:,1) Conv(:,2)];

    titles = {'Time(s)','Avg Current (A)','Avg Potential (V)','Time (s)',...
        'Co (mol/cm3)','Time (s)','Cr (mol/cm3)','Time (s)','Conv Current
(A)','Diffusion(cm^2/s)'};
    else
        xlsfile = 'Convoluted_Current_Data_Not_Averaged.xlsx';
        Data = [Time_corr(1:index) Current_avg(1:index)
Potential_avg(1:index) Time_corr(1:index) Cr Time_corr(1:index) Co'
Time_corr(1:index) Conv(:,2)];
        titles = {'Time(s)','Current (A)','Potential (V)','Time (s)',...
```

```
        'Co (mol/cm3)','Time (s)','Cr (mol/cm3)','Time (s)','Conv Current
(A/s^1/2^)','Diffusion(cm^2/s)'};
    end
xlswrite(xlsfile,titles,1,'A1')
xlswrite(xlsfile,Data,1,'A2')
xlswrite(xlsfile,D,1,'J2')

h=msgbox('Finished!');
```

Appendix A-3: MATLAB code for performing non-linear regression to curve fit cyclic voltammetry data: Program uses the output of the convolution program for the concentration of the electroactive species. The code was written by Prof. S. Nudehi.

```
clear all
close all
clc
format long

%% READ THE EXCEL DATA
% Sheet_Name='Comsol_DATA_Rev';
% Sheet_Page=1;
% Sheet_Range='A2:G16279';
% Data=xlsread(Sheet_Name,Sheet_Page,Sheet_Range);
%%

%% READ THE EXCEL DATA

Sheet_Name='CV data 3_23_16';
Sheet_Page=12;
Sheet_Range='A2:I3301';
Data=xlsread(Sheet_Name,Sheet_Page,Sheet_Range);



%% EXCTRACT I, CO CR

time=Data(:,1);
time(isnan(time))=[];

current=Data(:,2);
current(isnan(current))=[];

voltage=Data(:,3);
voltage(isnan(voltage))=[];

electrode_r=0. 01;
subplot(2,2,1)
plot(voltage,current)
title('experimental data')
grid on

xlabel('E (volts)')
ylabel('Current (Amps)')
index=0;
for i=time',
  index=index+1;
  r= min(find(Data(:,4)==i));
  Ca(index)=Data(r,5);

  r= min(find(Data(:,6)==i));
  Cb(index)=Data(r,7);
end
```

```
CA=Ca(:);
CB=Cb(:);
Half_time=length(CA);


subplot(2,2,2)
plot(voltage(1:Half_time),[CA(1:Half_time), CB(1:Half_time)])
xlabel('E (volts)')
ylabel('Ca , Cb (mole/m^3)')
grid on
title('experimental data:Concentrations')

ydata=current(1:Half_time);% [i]
xdata=[voltage(1:Half_time),CA(1:Half_time), CB(1:Half_time)];
%   [E(V)  , Co (mole/m^3)  ,Cr (mole/m^3)]

%% CONSTANTS
     F=96485. 3365; % s A / mol
     R=8. 3144621; %J/mol-K
     T=295; % K
    % A=0. 287e-4; %m^2
     A=8. 64; % cm^2
    % Ef=0; % Volts
     f=F/(R*T);
     n= 1; %mole of electrons per mole of products
%% CURVE_FIT SETUP
  options = optimoptions('lsqcurvefit');
  options. TolX = 1e-9;
  options. MaxIter = 10000;
  options. TolFun=1e-6;
  options. MaxFunEvals=1000;
  %options. Algorithm='levenberg-marquardt';
%% CURVE_FIT COMMAND
x = lsqcurvefit(@myfun2,[1,1,0], xdata, ydata,[0,0,-inf],[inf,
1,inf],options);
%% PLOT THE RESULTS
Y_Reg = -n*F*A*x(1)*(xdata(:,2). *exp(-x(2)*f*(xdata(:,1)-x(3)))- . . .
     xdata(:,3). *exp((1-x(2))*f*(xdata(:,1)-x(3))));
   k0=x(1)
   alpha=x(2)
   Ef=x(3)

   subplot(2,2,3)

% x(2)=0. 5;
% x(1)=1000;
%
% Y_Reg = F*A*x(1)*(xdata(:,2). *exp(-x(2)*f*(xdata(:,1)-Ef))- . . .
%     xdata(:,3). *exp((1-x(2))*f*(xdata(:,1)-Ef)));

plot(voltage(1:Half_time),ydata,voltage(1:Half_time),Y_Reg,'*k')
%legend('Exp. ', 'Fitted Data')
xlabel('E (volts)')
ylabel('Current (Amps)')
grid on
```

```
title (['k0=',num2str(x(1)),' ' '\alpha =',num2str(x(2)), ' ', 'Ef= '
num2str(x(3))])

 subplot(2,2,4)

 plot(log( CA(1:Half_time). / CB(1:Half_time)), voltage(1:Half_time))

 title('Nernst Equation')
 xlabel('Log(Ca/Cb)')
 ylabel('E(volts)')
 grid on

%
% figure
% a=0. 5;
% K=1000;
% Y2 = F*A*K*(xdata(:,2). *exp(-a*f*(xdata(:,1)-Ef))- . . .
%     xdata(:,3). *exp((1-a)*f*(xdata(:,1)-Ef)));
%  plot(voltage(1:Half_time),ydata,voltage(1:Half_time),Y2,'m')
%  legend('experiment','fitted data using the actual value')
%  xlabel('E(volts)')
%  ylabel('Current(A)')
%
```